Estimating Heat-transport and Time-delays in a Heat Exchanger

Sandra Hamze[1], Emmanuel Witrant[1], Delphine Bresch-Pietri[2], and Clement Fauvel[1,3]

***Abstract*— Transport and heat exchange phenomena occurring in a heat exchanger can be modeled as first-order hyperbolic partial differential equations (PDEs). Reformulating these equations as a time-delay system preserves the infinite-dimensional property of the system, yet decreases its mathematical complexity. Using a space-averaging technique and the method of characteristics, this paper proposes a time-delay system modeling of the flow temperatures of a heat exchanger. We propose to use a gradient-descent optimization method to estimate the parameters of this time-delay system, using boudary measurements of temperature in the heat exchanger. The interest of this approach is emphasized with experimental data obtained from the test-bench.**

I. INTRODUCTION

Time delay is a phenomenon encountered in many dynamic processes involving transfer of mass or energy. It naturally occurs in the interconnections of different parts of a system, as propagation of matter is not instantaneous. In particular, it occurs in tubular heat exchangers, which are very common devices in industry. These devices permit heat exchange between two fluids separated by a wall and circulating in opposite or, less often, in similar directions. Multi-flow transport phenomena, such as those encountered in a heat exchanger, although previously modeled as a first-order transfer function featuring delay [1], are better described by two first-order hyperbolic PDEs which better implicate the physical balance laws (see [2]). In the case of a tubular heat exchanger, for instance, two hyperbolic PDEs which take into consideration the temperature evolution of both fluids, the one in the internal tube as well as the one in the external tube are far more realistic than a single equation covering only the internal temperature evolution. Hence, recasting these hyperbolic PDEs as a time-delay system can be interesting as it preserves its infinite-dimensional property but also decreases its mathematical complexity, hence easing the design of a real-time control strategy.

In order to deal with hyperbolic PDE equations, different methods were presented in the literature. [3] for example replaces the PDEs representing a heat exchanger with sets of nonlinear ordinary differential equations with delayed inputs, each of these sets attributed to a section of the heat exchanger. Laplace transformation and numerical solutions of the PDE were also proposed in [4], [5], [6]. However, these numerical solutions exhibit convergence and stability issues. [7] on the other hand uses an analytical approach and a physical lumping approach with time delay at certain positions of the heat exchanger in order to deal with the flow and wall dynamics. However, the drawback of this methodology is its relative complexity order due to the division of the exchanger in cells.

In this paper, we represent the transport and heat exchange phenomena in a heat exchanger as coupled first-order hyperbolic PDEs. We propose to reformulate them as delay equations using the method of characteristics (see for example [8] or [9], [10] for an application in fluid networks, and [11] for an application in power lines). In order to ease this reformulation, we decouple the equations by using spatial-lumping. We then use a gradient-descent optimization method to estimate the parameters of the corresponding time-delay system (dynamics coefficients and time-delay). The interest of this technique is illustrated on experimental data.

This paper is organized as follows. Section II presents the model of hyperbolic PDEs, which serves as the reference model, and formulates the estimation problem. In section III, we detail the reformulation as a time-delay system before presenting in section IV the gradient-descent identification technique. Section V discusses the merits of this approach on experimental data obtained from a test bench. Finally, section VI concludes the paper with directions of future work.

II. PDE MODEL AND PROBLEM FORMULATION

A scheme of the tubular structure of the considered heat exchanger is shown in Figure 1. It shows two volumes of length L separated by a wall. In the top volume, a hot fluid of temperature T^H circulates in the rightward direction and, in the bottom volume, a cold fluid of temperature T^C circulates in the leftward direction. Heat exchange takes place between the two fluids through the wall separating the two tubes. T^{γ}_{in}

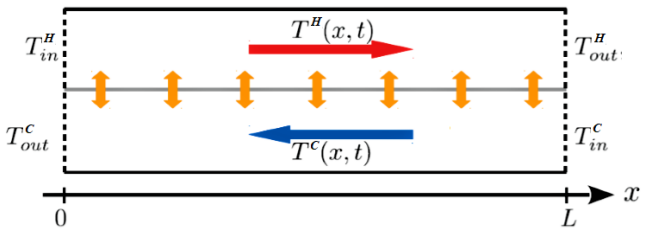

Fig. 1. Schematic representation of a heat exchanger

[1]Sandra HAMZE, Emmanuel WITRANT, and Remy JACCAZ are with Univ. Grenoble Alpes, CNRS, Grenoble INP, GIPSA-Lab, 38000 Grenoble, France
Email: Sandra.Hamze@gipsa-lab.grenoble-inp.fr
[2]Delphine BRESCH-PIETRI is with MINES Paristech, PSL Research University, CAS-Centre Automatique et Systemes, 60 bd Saint Michel, 75006 Paris, France
[3]Clement FAUVEL is with CEA-Commissariat a l'energie atomique et aux energies alternatives, 38000 Grenoble, France

and T^{γ}_{out} ($\gamma = (H, C)$) are the respective temperatures of the fluid at the entrance of the tube and at its exit.

We consider the following assumptions from [12]:

- the flow is one-dimensional (along an axis called x), with the hot fluid direction considered as positive.
- the heat diffusion through the tubes of the heat exchanger is negligible;
- convection between the two fluids is the only heat exchange taking place;
- the external walls of the heat exchanger are adiabatic and no heat exchange between the heat exchanger and its surrounding environment takes place;
- the heat transfer coefficient is constant.

Under these assumptions, the temperature dynamics of the heat exchanger can be represented as the following system of coupled hyperbolic first order PDEs [2][12]

$$\frac{\partial T^H(x,t)}{\partial t} + c_1 \frac{\partial T^H(x,t)}{\partial x} = -d_1(T^H(x,t) - T^C(x,t)) \tag{1a}$$

$$\frac{\partial T^C(x,t)}{\partial t} - c_2 \frac{\partial T^C(x,t)}{\partial x} = d_2(T^H(x,t) - T^C(x,t)) \tag{1b}$$

T^H is the distributed temperature of the hot fluid, T^C is that of the cold fluid, c_1, d_1, c_2, and d_2 are constant positive coefficients, x is the spatial coordinate spanning interval $[0, L]$, and t is the time coordinate spanning interval $[t_0, \infty)$. The corresponding boundary and initial conditions are

$$T^H(0,t) = T^H_{in}(t) \text{ and } T^C(L,t) = T^C_{in}(t)$$

$$T^H(x,0) = T^H_0(x) \text{ and } T^C(x,0) = T^C_0(x)$$

This model illustrates the total convective heat transfer rate ($hA\Delta T$) as the summation of the rate of heat transfer of the pipe in time $\left(\rho V C_p \frac{\partial T}{\partial t}\right)$ and the rate of heat transfer to the wall of the pipe $\left(\dot{M} C_p \frac{\partial T}{\partial x}\right)$. ρ, V, C_p, $\dot{M}$, h, A, and ΔT are respectively the density of the fluid, volume of pipe, specific heat, mass flow rate, convection exchange coefficient, heat transfer surface area, and the temperature gradient. This implies that the transport and heat exchange parameters c_1, d_1, c_2, and d_2 are highly uncertain (as d_1 and d_2 depend on the convection exchange coefficient which reveals troublesome to determine). Therefore, we aim at obtaining an estimation technique using only boundary measurements of the temperatures $T^H_{in}(t)$, $T^C_{in}(t)$, $T^H(L,t)$, and $T^C(0,t)$. Before detailing this point, we first focus on a time-delay approximation of this model.

III. FROM PDE TO TIME-DELAY EQUATIONS

Consider the coupled first-order hyperbolic PDE system (1) representing the heat exchanger dynamics. In order to decouple these equations, the space-averaging technique presented in [10] is used to replace $T^C(x,t)$ in equation (1a) by the average

$$\frac{T^C_{in}(t)+T^C_{out}(t)}{2} = \frac{T^C(L,t)+T^C(0,t)}{2} \triangleq \frac{f(t)}{2}$$

and to replace $T^H(x,t)$ in equation (1b) by the average

$$\frac{T^H_{in}(t)+T^H_{out}(t)}{2} = \frac{T^H(0,t)+T^H(L,t)}{2} \triangleq \frac{g(t)}{2}$$

Let's denote $T^H_x = \frac{\partial T^H(x,t)}{\partial x}$ and $T^H_t = \frac{\partial T^H(x,t)}{\partial t}$ (similarly for T^C). The system dynamics can hence be expressed as

$$T^H_t + c_1 T^H_x = -d_1 T^H(x,t) + \frac{d_1}{2} f(t) \tag{2a}$$

$$T^C_t - c_2 T^C_x = -d_2 T^C(x,t) + \frac{d_2}{2} g(t) \tag{2b}$$

As the two equations belong to the same class of models, only the first equation is discussed hereafter.

Following the method of characteristics presented in [13] which is used to transform a PDE system into a set of ordinary differential equations (ODEs), we consider a point $(x,t) \in [0, L] \times [t_0, \infty)$ and define the function

$$z(\theta) = T^H(c_1\theta + x, \theta + t) \tag{3}$$

$C = \{x(\theta), t(\theta), z(\theta)\}$ is the characteristic curve which passes through point (x,t) and satisfies the ODEs:

$\frac{dx(\theta)}{d\theta} = c_1$, $\frac{dt(\theta)}{d\theta} = 1$, and $\frac{dz(\theta)}{d\theta}$ obtained using (2a) as:

$$\begin{aligned}\frac{dz(\theta)}{d\theta} &= c_1 T^H_x(c_1\theta + x, \theta + t) + T^H_t(c_1\theta + x, \theta + t) \\ &= -d_1 T^H(c_1\theta + x, \theta + t) + \frac{d_1}{2} f(\theta + t) \\ &= -d_1 z(\theta) + \frac{d_1}{2} f(\theta + t)\end{aligned} \tag{4}$$

Hence, the distributed temperature of the hot fluid is

$$\begin{aligned}T^H(x,t) =& T^H_{in}\left(t - \frac{x}{c_1}\right) e^{-d_1 \frac{x}{c_1}} \\ &+ \frac{d_1}{2} e^{-d_1 \frac{x}{c_1}} \int_0^{\frac{x}{c_1}} f\left(\eta + t - \frac{x}{c_1}\right) e^{d_1 \eta} d\eta\end{aligned} \tag{5}$$

By evaluating (5) at $x = L$, the output temperature $T^H(L,t)$ is thus obtained as

$$\begin{aligned}T^H(L,t) =& T^H_{in}\left(t - \frac{L}{c_1}\right) e^{-d_1 \frac{L}{c_1}} \\ &+ \frac{d_1}{2} e^{-d_1 \frac{L}{c_1}} \int_0^{\frac{L}{c_1}} f\left(\eta + t - \frac{L}{c_1}\right) e^{d_1 \eta} d\eta\end{aligned} \tag{6}$$

Similarly, from (2b), one obtains

$$\begin{aligned}T^C(x,t) =& T^C_{in}\left(t - \frac{L-x}{c_2}\right) e^{-d_2 \frac{L-x}{c_2}} \\ &+ \frac{d_2}{2} e^{-d_2 \frac{L-x}{c_2}} \int_0^{\frac{L-x}{c_2}} g\left(\eta + t - \frac{L-x}{c_2}\right) e^{d_2 \eta} d\eta\end{aligned} \tag{7}$$

By evaluating (7) at the other boundary of the cold tube at $x = 0$, the output temperature $T^C(0,t)$ is obtained as

$$\begin{aligned}T^C(0,t) =& T^C_{in}\left(t - \frac{L}{c_2}\right) e^{-d_2 \frac{L}{c_2}} \\ &+ \frac{d_2}{2} e^{-d_2 \frac{L}{c_2}} \int_0^{\frac{L}{c_2}} g\left(\eta + t - \frac{L}{c_2}\right) e^{d_2 \eta} d\eta\end{aligned} \tag{8}$$

Thus, (5)-(8) are time-delay equations depending only on past values of the boundary measurements.

IV. ESTIMATION OF THE PARAMETERS OF THE TIME-DELAY EQUATIONS

Time-delay equations (6) and (8) are now used to identify the vector $\kappa = \begin{bmatrix} c_1 & d_1 & c_2 & d_2 \end{bmatrix}$, and hence the time delays $\frac{L}{c_1}$ and $\frac{L}{c_2}$. The optimization method we propose to use is a gradient-descent algorithm, such as the one proposed in [14] for the optimal control of time-delay systems. The objective is to minimize over time the squared error ε

$$\varepsilon = \begin{bmatrix} T^H{}_{measured} - T^H{}_{model}(L,\cdot) \\ T^C{}_{measured} - T^C{}_{model}(0,\cdot) \end{bmatrix} \tag{9}$$

which is defined as the difference between the test bench output temperatures (measured temperatures) and the ones provided by the model (6) and (8).

The gradient-descent method is summarized below. Its objective is to find the optimal vector κ^* that minimizes the cost function defined as

$$J(\hat{\kappa},t) = \frac{1}{2t_f}\int_0^{t_f} \varepsilon(\hat{\kappa},t)^T Q \varepsilon(\hat{\kappa},t) dt \tag{10}$$

where t_f is a given time horizon, Q is a weighting matrix, and $\hat{\kappa}$ is an estimate of the parameter vector κ, whose derivative is defined as

$$\dot{\hat{\kappa}} = -\alpha(\hat{\kappa},t)\nabla J(\hat{\kappa},t) \tag{11}$$

The gradient is computed as

$$\nabla J(\hat{\kappa},t) = -\frac{1}{t_f}\int_0^{t_f} \varepsilon(\hat{\kappa},t)^T Q S(\hat{\kappa},t) dt \tag{12}$$

where $S = \begin{bmatrix} \frac{\partial y}{\partial c_1} & \frac{\partial y}{\partial d_1} & \frac{\partial y}{\partial c_2} & \frac{\partial y}{\partial d_2} \end{bmatrix}$ is the sensitivity function, $y = [T^H(L,t) \;\; T^C(0,t)]^T$, and $\alpha(\hat{\kappa},t)$ is the step obtained from Newton's method [15] and is defined as

$$\alpha(\hat{\kappa},t) = \left(\frac{1}{t_f}\int_0^{t_f} S(\hat{\kappa},t)^T Q S(\hat{\kappa},t) dt + \upsilon I\right)^{-1} \tag{13}$$

with υ a positive constant acting as a tuning parameter.

By definition, one has

$$S_1 = \frac{\partial y}{\partial c_1} = \begin{bmatrix} \frac{\partial T^H(L,t)}{\partial c_1} \\ 0 \end{bmatrix} \qquad S_2 = \frac{\partial y}{\partial d_1} = \begin{bmatrix} \frac{\partial T^H(L,t)}{\partial d_1} \\ 0 \end{bmatrix}$$
$$S_3 = \frac{\partial y}{\partial c_2} = \begin{bmatrix} 0 \\ \frac{\partial T^C(0,t)}{\partial c_2} \end{bmatrix} \qquad S_4 = \frac{\partial y}{\partial d_2} = \begin{bmatrix} 0 \\ \frac{\partial T^C(0,t)}{\partial d_2} \end{bmatrix} \tag{14}$$

in which

$$\begin{aligned} \frac{\partial T^H(L,t)}{\partial c_1} = & -\frac{L d_1}{2{c_1}^2} f(t) + \frac{L}{{c_1}^2} e^{-d_1\frac{L}{c_1}} \times \\ & \left(\frac{dT^H_{in}\left(t-\frac{L}{c_1}\right)}{dt} + d_1 T^H_{in}\left(t-\frac{L}{c_1}\right) \right. \\ & + \frac{d_1^2}{2}\int_0^{\frac{L}{c_1}} f\left(\eta + t - \frac{L}{c_1}\right) e^{d_1\eta} d\eta \\ & \left. + \frac{d_1}{2}\int_0^{\frac{L}{c_1}} \frac{df\left(\eta + t - \frac{L}{c_1}\right)}{dt} e^{d_1\eta} d\eta \right) \end{aligned} \tag{15}$$

$$\begin{aligned} \frac{\partial T^H(L,t)}{\partial d_1} = & \; T^H_{in}\left(t-\frac{L}{c_1}\right)\left(\frac{-L}{c_1}\right) e^{-d_1\frac{L}{c_1}} \\ & + \frac{c_1 - L d_1}{2c_1} e^{-d_1\frac{L}{c_1}} \int_0^{\frac{L}{c_1}} f\left(\eta + t - \frac{L}{c_1}\right) e^{d_1\eta} d\eta \\ & + \frac{d_1}{2} e^{-d_1\frac{L}{c_1}} \int_0^{\frac{L}{c_1}} f\left(\eta + t - \frac{L}{c_1}\right)(\eta) e^{d_1\eta} d\eta \end{aligned} \tag{16}$$

S_3 and S_4 have the same form as S_1 and S_2 respectively, except that c_1 is replaced by c_2, d_1 is replaced by d_2, and $f(\cdot)$ is replaced by $g(\cdot)$. Note that the integrals in the sensitivities can be estimated in practice using the trapezoidal rule, and the time derivatives $\frac{df(.)}{dt}$ and $\frac{T^H_{in}(.)}{dt}$ can be approximated in practice using a Backward Euler discretization. Section V shows that the effect of this approximation is not substantial and that noise sensitivity is fairly resulting from the experimental measurements.

V. EXPERIMENTAL SETUP AND RESULTS

A. Experimental Setup

The proposed approach is evaluated on a heat exchanger test-bench available in GIPSA-lab, Grenoble, France. As shown in Figure 2, it consists of a hot tank (equipped with an immersed heater which heats the water up to a target temperature), a cold tank, and a heat exchanger which is a tubular structure made of two concentric tubes, an external tube in which the hot fluid circulates and an internal tube in which the cold fluid circulates. The surfaces of the tubes are designed to maximize the turbulence of the flows. In addition to that, it also consists of hot fluid and cold fluid pumps, manual and automatic valves to direct the flows, and various sensors of temperature, pressure, and volumetric flow rate. The sensors provide the measurements of the temperature and the volumetric flow rate of each of the fluids at the entrances and exits of the exchanger. A fresh water source and the immersed heater allow controlling the temperatures at the entrances of the exchanger. In addition, the test bench is equipped with a target PC used for data acquisition and a host PC through which the user can communicate with the target PC using the XPC Target of Simulink. The exchanger is dimensioned according to the values provided in Table I. Hence, for a hot fluid temperature of $70°C$ and a flow

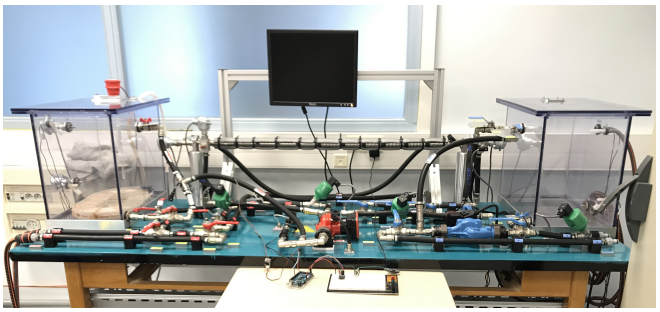

Fig. 2. Heat exchanger test bench in GIPSA-lab

rate of $0.2m^3/h$, a temperature difference of $10°C$ between the input and the output is expected, i.e. a theoretical heat capacity of $2.3kW$.

TABLE I

NOMINAL THERMAL SPECIFICATIONS OF THE HEAT EXCHANGER TEST-BENCH

	Flow Rate	T_{in}	T_{out}	Reynold's nb	Flow Type
Cold	0.2 m^3/h	$20°C$	$30°C$	8000	Turbulent
Hot	0.2 m^3/h	$70°C$	$60°C$	5500	Transitional

B. Experimental Results

Two sets of experiments are used, one for identification and another for validation. The identification experiment is held at around $T_{in}^H = 40°C$, and mass flow rates $\dot{m} = 260$ L/hr. The validation experiment is a concatenation of two experiments held at a temperature $T_{in}^H = 60°C$, and mass flow rates $\dot{m} = 260$ L/hr. The difference between the first and the second validation experiment is that, in the first experiment, a disturbance is applied on the entrance of the hot circuit (T_{in}^H) and no disturbance is applied on the cold circuit, whereas the second experiment consists in the reverse, that is a disturbance is applied on the entrance of the cold circuit (T_{in}^C) and no disturbance is applied on the hot circuit. The optimization problem is set with the following parameters:

- Initial set of parameters $\kappa_0 = \begin{bmatrix}0.01 & 0.001 & 0.01 & 0.001\end{bmatrix}$
- $Q = \begin{bmatrix}4 & 0\\ 0 & 10\end{bmatrix}$
  A higher weight Q_{22} is attributed to the cold temperature error because, in the experimental setup, the hot tube is the external tube. Therefore, the hot temperature can be subject to unmodelled exchange with the external environment despite the isolation.
- $\upsilon = 10^{-9}$
- $\|\nabla J\| \leq 10^{-6}$ is a stop condition of the optimization.

The primary concern is to show that the time-delay model is able to reproduce the same output as the PDE system. For this sake, a first estimation of the transport and exchange parameters is done using the discretized PDE system and the gradient-descent estimation method derived previously. The estimated parameters are shown in Table II.

TABLE II

PARAMETERS ESTIMATED WITH THE PDE MODEL

c_1 (m/s)	d_1 (W/Jm)	c_2 (m/s)	d_2 (W/Jm)
0.12144	0.023693	0.17998	0.029412

Using these parameters, the PDE and the time-delay system are simulated with the measured input temperatures and compared with the outflows measurements provided by the test-bench experiments. Figure 3 corresponds to the identification experiment, with Figure 4 showing its corresponding absolute error on the whole time-scale. Figures 5 and 6 show

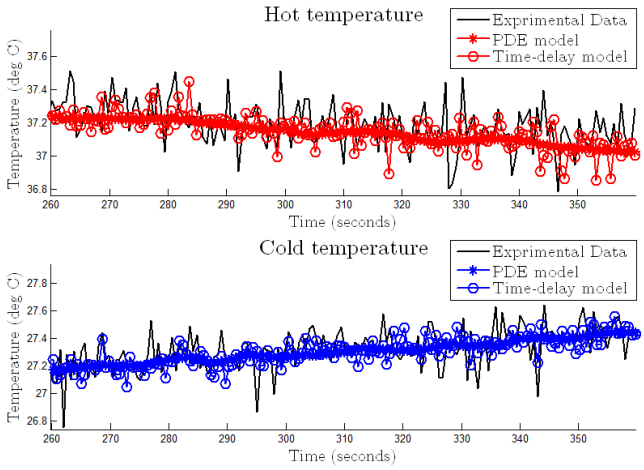

Fig. 3. Comparison of the PDE and the time-delay models with respect to the experimental data - identification experiment

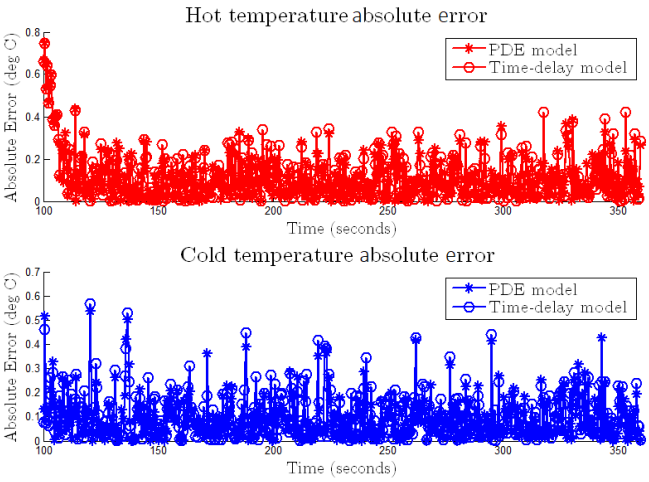

Fig. 4. Absolute errors of PDE and time-delay models with respect to the experimental data - identification experiment

the same results on the validation experiments. The mean-squared averaged error

$$\frac{1}{N}\sum_{i=1}^{N}(T^{\gamma}_{measured} - T^{\gamma}_{model})^2 \tag{17}$$

corresponding to the experiments simulated with the parameters estimated from the PDE model is shown in Table III.

TABLE III

MEAN-SQUARED AVERAGE ERROR

Experiment set	Identification		Validation	
Fluid	Hot	Cold	Hot	Cold
PDE	0.0234	0.019	3.3333	2.3533
Time-delay	0.0275	0.0237	4.3190	2.5425

The simulation results show the credibility of the PDE and the time-delay models as the error separating them from the experimental data is low, especially in the identification experiment. In addition to that, the error separating each of

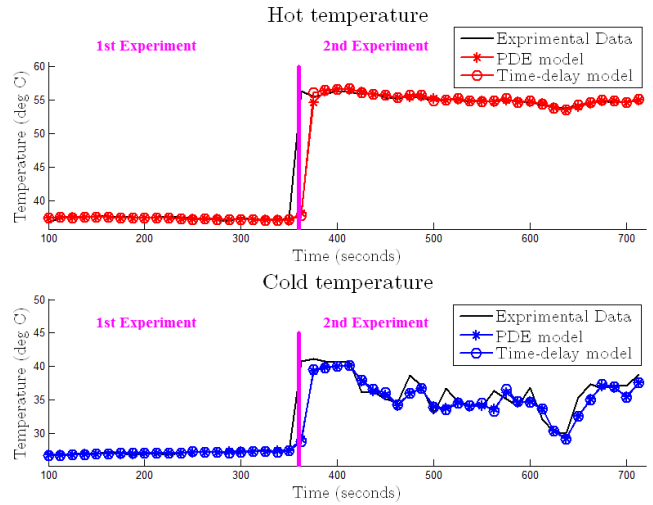

Fig. 5. Comparison of the PDE and the time-delay models with respect to the experimental data - validation experiment

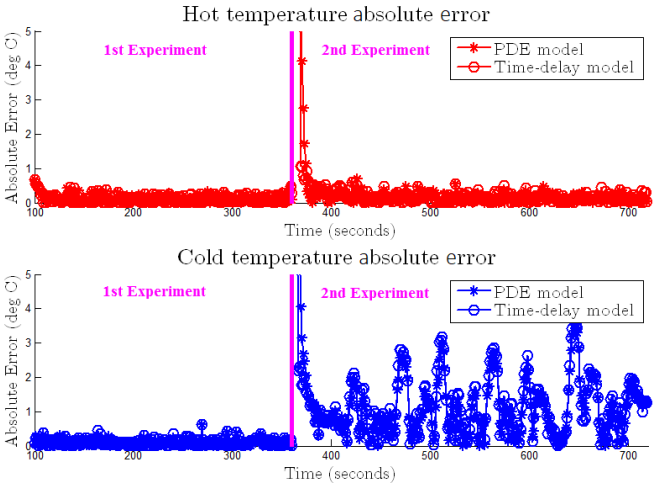

Fig. 6. Absolute errors of PDE and time-delay models with respect to the experimental data - validation experiment

the PDE and the time-delay models from the experiment is very close indicating a very slight difference between them, which illustrates the adequacy of the averaging assumption.

TABLE IV

PARAMETERS ESTIMATED WITH THE TIME-DELAY MODEL

$c_1\ (m/s)$	$d_1\ (W/Jm)$	$c_2\ (m/s)$	$d_2\ (W/Jm)$
15.9021	3.14237	16.1599	2.59372

The following step is to identify the system using the time-delay model, i.e. equations (6) and (8). The results are shown in Table IV. Although the estimated parameters are quite different from those estimated in the case of the PDE system, the simulation results tend to imply that this new set of parameters is also valid. Indeed simulating the PDE model and the time-delay model using these parameters, we obtain the results shown in Figure 7 for the identification

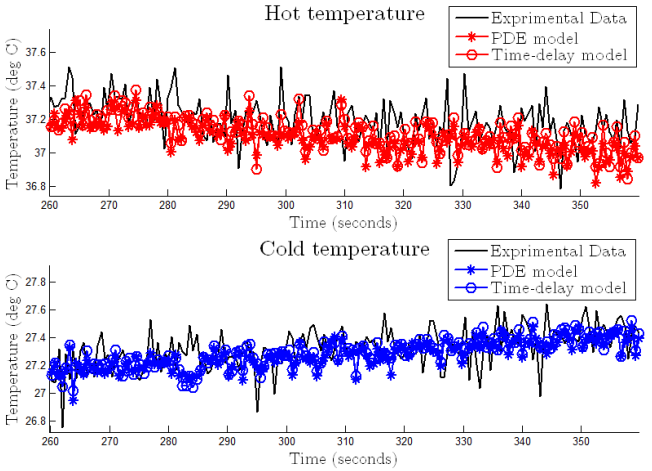

Fig. 7. Comparison of the PDE and the time-delay models with respect to the experimental data - identification experiment

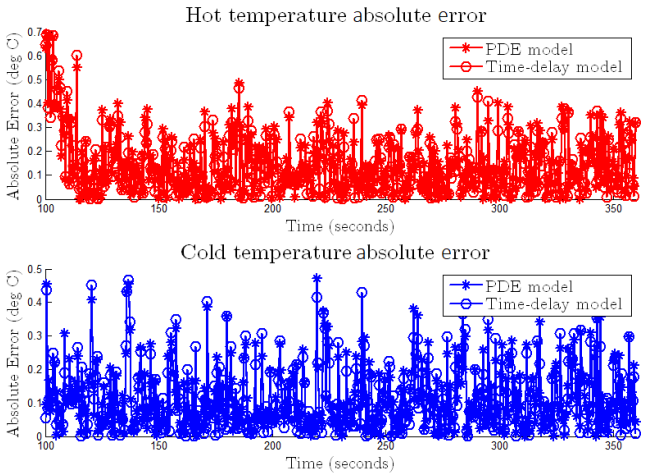

Fig. 8. Absolute errors of PDE and time-delay models with respect to the experimental data - identification experiment

experiment and those shown in Figure 9 for the validation experiment. The mean-squared averaged error corresponding to the experiments simulated with the parameters estimated from the time-delay model is summarized in Table V.

TABLE V

MEAN-SQUARED AVERAGE ERROR

Experiment set	Identification		Validation	
Fluid	Hot	Cold	Hot	Cold
PDE	0.0357	0.0259	0.0655	0.3947
Time-delay	0.0335	0.0252	0.0862	0.3921

These results show that the two models have a high level of similarity and a good level of fit with the experimental data. This can also be seen in Table V and Figures 8 and 10 which show low absolute errors in case of the identification experiment as well as the validation experiment.

Additionally, by comparing Tables III and V, we can notice that the mean-squared error obtained on the iden-

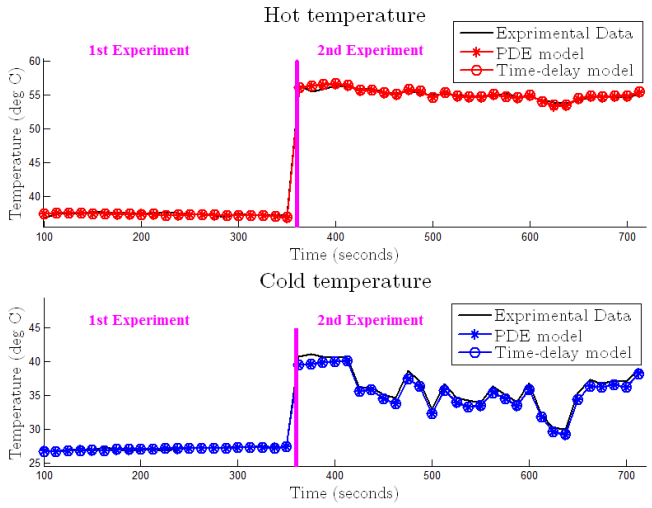

Fig. 9. Comparison of the PDE and the time-delay models with respect to the experimental data - validation experiment

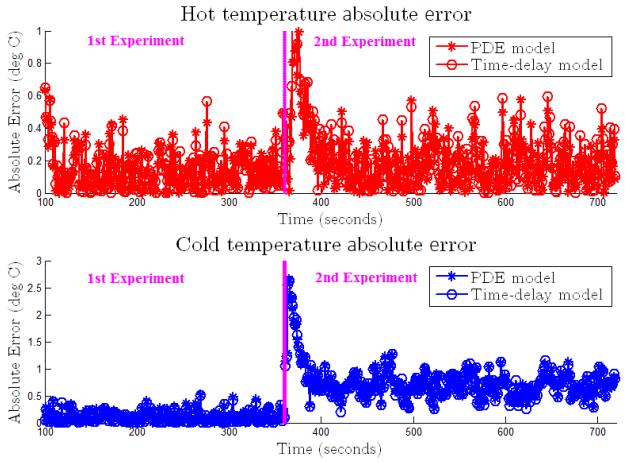

Fig. 10. Absolute errors of PDE and time-delay models with respect to the experimental data - validation experiment

tification experiment with the parameters estimated from the PDE system is almost equal to that recorded on the same experiment but with the parameters estimated from the time-delay system. Although this implies that the estimation algorithm works similarly on both models, the mean-squared errors corresponding to the validation experiment are much better in the case when the estimation is done using the time-delay model. Moreover, a time-save of 98% can be noted when launching the estimation algorithm using the time-delay system implying that the time-delay system is more adequate than the PDE model to be used for estimation using gradient-descent algorithm.

Finally, Tables II and IV show that the parameter vector estimated using the PDE model is far from that estimated using the time-delay model. However, we can notice that the ratio $\frac{c_1}{d_1} = 5.12$ from Table II is almost equal to the ratio $\frac{c_1}{d_1} = 5.06$ from Table IV. The same remark can also be attributed to the ratio $\frac{c_2}{d_2}$. This might be explained by the simulation results depicted in Figures 3 and 7 showing that the PDE system and the time-delay model represent more accurately the steady-state behavior of the model rather than its transient state.

VI. CONCLUSIONS

A space-averaging technique is proposed in this paper to allow decoupling first-order hyperbolic PDEs representing a heat exchanger and reformulating them as a time-delay system. Its merits were illustrated on experimental data and the time-delay model showed being more efficient for identification purposes than the original PDEs. A future scope of research lies in exploiting the identified time-delay model for control purposes.

REFERENCES

[1] H. Thal-Larsen, "Dynamics of heat exchangers and their models," *Journal of Basic Engineering*, vol. 82, no. 2, pp. 489–500, 1960.

[2] F. Bonne, M. Alamir, and P. Bonnay, "Nonlinear observer of the thermal loads applied to the helium bath of a cryogenic Joule-Thompson cycle," *Journal of Process Control*, vol. 24, pp. 73–80, 2014.

[3] J. O. M. Bakosova, M. Kacur, "Control of a tubular heat exchanger," in *18th International Conference on Process Control*, Tatranska Lomnica, Slovakia, June 2011, pp. 338–343.

[4] S. Alotaibi, M. Sen, B. Goodwine, and K. Yang, "Controllability of cross-flow heat exchangers," *International Journal of Heat and Mass Transfer*, vol. 47, pp. 913–924, 2004.

[5] F. Romie, "Transient response of the counter-flow heat exchanger," *ASME J. Heat Transfer*, vol. 106, no. 3, pp. 620–626, 1984.

[6] Y. X. Roetzel W, "Transient/response of parallel and counter-flow heat exchangers," *J. Heat Transfer*, vol. 114, no. 2, pp. 510–512, 1992.

[7] D. Debeljkovic and G. Simeunovic, "Modelling, simulation and dynamic analysis of the time delay model of the recuperative heat exchange," *Tehnika-Masinstivo*, vol. 65, no. 3, pp. 407–413, 2016.

[8] J. C. Strikwerda, *Finite difference schemes and partial differential equations*, 2nd ed. Philadelphia, USA: Siam, 2004, vol. 88.

[9] I. Karafyllis and M. Krstic, "On the relation of delay equations to first-order hyperbolic partial differential equations," *ESAIM:COCV*, vol. 20, no. 3, pp. 894–923, 2014.

[10] D. Novella-Rodriguez, E. Witrant, and O. Sename, "Control-oriented modeling of fluid networks: A time-delay approach," in *Recent Results on Nonlinear Delay Control Systems*. Springer, 2016, pp. 275–289.

[11] K. L. Cooke and D. K. Krumme, "Differential-difference equations and nonlinear initial-boundary value problems for linear hyperbolic partial differential equations," *Journal of Mathematical Analysis and Applications*, vol. 24, no. 2, pp. 372–387, 1968, .

[12] F. Zobiri, E. Witrant, and F. Bonne, "PDE observer design for counter-current heat flows in a heat-exchanger," *IFAC-PapersOnline*, vol. 50, no. 1, pp. 7127–7132, 2017, .

[13] L. C. Evans, *Partial Differential Equations*, 2nd ed. Providence, Rhode Island: American Mathematical Society, 2010, vol. 19.

[14] E. Witrant, D. Georges, and C. C. De Wit, "Optimal control design for the stabilization of network controlled systems," in *Proceedings of the 2006 American Control Conference*. Minneapolis, Minnesota, USA: IEEE, June 2006, pp. 2777–2782.

[15] K. Madsen, H. B. Nielsen, and O. Tingleff, "Methods for non-linear least squares problems," Richard Petersens Plads, Building 321, DK-2800 Kgs. Lyngby, p. 56, 1999. [Online]. Available: http://www2.imm.dtu.dk/pubdb/p.php?660